AD/A-005 004

HEAT PIPE COPPER VAPOR LASER

Robert J. L. Chimenti

Exxon Research and Engineering Company

Prepared for:

Office of Naval Research
Advanced Research Projects Agency

November 1974

EXXON RESEARCH AND ENGINEERING COMPANY

GRU.2.BEOA.74

HEAT PIPE COPPER VAPOR LASER

Final Technical Report

November 1974

ARPA Order Number:	1806, Amendment 9
Program Code:	3E90
Contractor:	Exxon Research and Engineering Company
Effective Date of Contract:	1 February 1973
Contract Expiration Date:	30 June 1974
Amount of Contract:	$159,775
Contract Number:	N00014-73-C-0317
Principal Investigator:	Robert J. L. Chimenti (201-474-2298)
Scientific Officer:	Director, Physics Program ONR
Short Title:	Heat Pipe Copper Vapor Laser

The views and conclusions contained in this document are those of the author and should not be interpreted as necessarily representing the official policies, either expressed or implied, of the Advanced Research Projects Agency or the U.S. Government.

Sponsored By

Advanced Research Projects Agency
ARPA Order 1806, Amendment 9

government research

P. O. BOX 8 ■ LINDEN, NEW JERSEY 07036

SUMMARY

The development of a high temperature copper vapor laser with vapor pressures above 1 torr has been limited, in part, by the lack of a vapor containment technique capable of cyclic operation to temperatures of 2000°C and compatible with a discharge configuration capable of the generation of high current, short risetime excitation. The program objective was the development of a copper vapor laser in which the copper was contained within a heat pipe and whose vapor density could be controlled by an inert gas.

The first part of the program involved the development and investigation of a heat pipe with copper as the working fluid. Successful operation of a heat pipe with graphite and tungsten as the materials of construction was obtained to temperatures of 2100°C. Both helium and argon were used for the control of the copper vapor pressure.

The second aspect of the program was the development of a discharge configuration capable of the production of high current, short risetime excitation in the vapor and compatible with the heat pipe structure. Toward these ends a class of transverse discharge configurations was developed which operated in the heat pipe and which produced excitation current pulses of thousands of amperes with a risetime of typically 10^{-8} seconds. Pulse generators were developed which were integral with the laser structure and had variable pulse repetition rates from one to 10^4 pulses per second.

In the third part of the program investigation of laser action obtained in the heat pipe was carried out. Laser action at both 0.5106μ and 0.5782μ was successfully demonstrated at temperatures between 1500°C and 1900°C. The upper operating temperature limit corresponds to a copper vapor pressure of nearly 15 torr. This is the highest laser operating pressure thus far reported. Laser action was obtained in pure copper as well as with inert gas pressures to 250 torr. Output power in excess of 75 kW from a small volume has been demonstrated in preliminary experiments. This corresponded to an energy density of $50\mu J\text{-}cm^{-3}$. Multiple laser pulses resulting from a single excitation pulse have been observed at temperatures above 1700°C with pulse widths less than 2.5 nsec (bandwidth limited).

While the major technical objectives have been achieved, further work is required in the improvement of the structural integrity of the heat pipe under conditions of thermal cycling. Alternate discharge configurations should be explored in an effort to increase the current density in the active volume.

UNCLASSIFIED

SECURITY CLASSIFICATION OF THIS PAGE (When Data Entered)

REPORT DOCUMENTATION PAGE

READ INSTRUCTIONS BEFORE COMPLETING FORM

1. REPORT NUMBER	2. GOVT ACCESSION NO. / 3. RECIPIENT'S CATALOG NUMBER
4. TITLE (and Subtitle) Heat Pipe Copper Vapor Laser	5. TYPE OF REPORT & PERIOD COVERED Final Report 1 February 1973-30 June 1974
	6. PERFORMING ORG. REPORT NUMBER GRU.2BEOA.74
7. AUTHOR(s) Robert J. L. Chimenti	8. CONTRACT OR GRANT NUMBER(s) N00014-73-C-0317
9. PERFORMING ORGANIZATION NAME AND ADDRESS Exxon Research and Engineering Company P.O. Box 8 - Government Research Laboratory Linden, New Jersey 07036	10. PROGRAM ELEMENT, PROJECT, TASK AREA & WORK UNIT NUMBERS ARPA Order No. 1806, Amend. 9 Program Code No. 3E90/11-15-72
11. CONTROLLING OFFICE NAME AND ADDRESS Physical Sciences Division Office of Naval Research Department of the Navy 800 N. Quincy St., Arlington, VA 22217	12. REPORT DATE November 1974
	13. NUMBER OF PAGES 43
14. MONITORING AGENCY NAME & ADDRESS(if different from Controlling Office) Same as Block 11	15. SECURITY CLASS (of this report) Unclassified
	15a. DECLASSIFICATION/DOWNGRADING SCHEDULE None

16. DISTRIBUTION STATEMENT (of this Report)

Approved for public release; distribution unlimited.

17. DISTRIBUTION STATEMENT (of the abstract entered in Block 20, if different from Report)

Same as Block 16

18. SUPPLEMENTARY NOTES

None

19. KEY WORDS (Continue on reverse side if necessary and identify by block number)

Metal Vapor Lasers, Heat Pipe, Electric Discharge

20. ABSTRACT (Continue on reverse side if necessary and identify by block number)

The development of a high temperature copper vapor laser with vapor pressures above 1 torr has been limited, in part, by the lack of a vapor containment technique capable of cyclic operation to temperatures of 2000°C and compatible with a discharge configuration capable of the generation of high current, short risetime excitation. The program objective was the development of a copper vapor laser

DD FORM 1 JAN 73 1473 EDITION OF 1 NOV 65 IS OBSOLETE

PRICES SUBJECT TO CHANGE

UNCLASSIFIED

SECURITY CLASSIFICATION OF THIS PAGE (When Data Entered)

in which the copper was contained within a heat pipe and whose vapor density could be controlled by an inert gas.

The first part of the program involved the development and investigation of a heat pipe with copper as the working fluid. Successful operation of a heat pipe with graphite and tungsten as the materials of construction was obtained to temperatures of 2100°C. Both helium and argon were used for the control of the copper vapor pressure.

The second aspect of the program was the development of a discharge configuration capable of the production of high current, short risetime excitation in the vapor and compatible with the heat pipe structure. Toward these ends a class of transverse discharge configurations were developed which operated in the heat pipe and which produced excitation current pulses of thousands of amperes with a risetime of typically 10^{-8} seconds. Pulse generators were developed which were integral with the laser structure and had variable pulse repetition rates from one to 10^4 pulses per second.

In the third part of the program investigation of laser action obtained in the heat pipe was carried out. Laser action at both 0.5106μ and 0.5782μ was successfully demonstrated at temperatures between 1500°C and 1900°C. The upper operating temperature limit corresponds to a copper vapor pressure of nearly 15 torr. This is the highest laser operating pressure thus far reported. Laser action was obtained in pure copper as well as with inert gas pressures to 250 torr. Output power in excess of 75 kW from a small volume has been demonstrated in preliminary experiments. This corresponded to an energy density of $50\mu J\text{-}cm^{-3}$. Multiple laser pulses resulting from a single excitation pulse have been observed at temperatures above 1700°C with pulse widths less than 2.5 nsec (bandwidth limited).

TABLE OF CONTENTS

LIST OF FIGURES

I. LASER ACTION IN ATOMIC COPPER VAPOR

A. Collisional and Radiative Processes Leading to Laser Action

A partial energy level diagram of the copper atom is shown in Figure 1. Laser action occurs at 0.5106μ and 0.5782μ between the $3d^{10}4p\ ^2P^o_{3/2,\ 1/2}$ and the $3d^9 4s^2\ ^2D_{5/2,3/2}$ levels in the neutral metal atom. The $4p\ ^2P^o$ upper laser levels are the first resonance levels in the copper atom and are coupled to the ground state by strong electric dipole transitions. The $4s^2\ ^2D$ lower laser levels are metastable against radiative decay, being of the same parity as the ground state. The atomic ground state consists of a single level and there are no other intermediate energy levels between the ground state and the laser levels. The laser transitions are partially forbidden since two simultaneous electron jumps from the 4p to 4s and 3d to 4s levels are involved. A consequence of the partially forbidden nature of the transition is that the radiative transition probability is relatively small. The spontaneous emission A-values (1) are presented in Figure 1.

It can be seen from the transition probabilities listed in Figure 1 that the branching ratios, for the $4s^2\ ^2D - 4p\ ^2P$ laser transitions are quite small. For example, only 1.2% of the excited $4p\ ^2P^o_{3/2}$ atoms which are produced would radiate on the 0.5106μ line at low pressure. In order to increase the laser transition branching ratio the density of ground state copper atoms must be sufficient to trap (2) the resonance radiation.

Excitation of the laser levels occur by a one-step, direct collision between an electron and a ground state copper atom. It is known that electron impact excitation cross-sections are largest between optically allowed levels (3). The excitation cross-sections to the $4p\ ^2P^o$ upper laser levels will then be greater than to the metastable lower laser levels for electron energies above a certain threshold value. Excitation cross-sections and excitation rates to the upper and lower laser levels as a function of the incident electron energy have been published by Leonard (4). The rates were computed by thermally averaging the product of the electron excitation cross-section with the electron velocity. For electron temperatures above 2 ev, a population inversion can be produced between the $4p\ ^2P^o$ and $4s^2\ ^2D$ levels. It should be pointed out, however, that use of a Maxwellian velocity distribution to calculate the inelastic rates of interest assumes that the net drift velocity of the plasma electrons is small compared with the mean thermal velocity. The implication is that the energy gained by the electrons between collisions in the applied electric field is small compared with the threshold energies for inelastic collisions. The situation is precisely the opposite, however, for the large value of the electric field which is applied to the vapor in the copper laser. Furthermore, recent measurements at JPL (5) show poor agreement with the calculated cross-sections.

In order to achieve the population inversion it is necessary that the risetime of the excitation pulse be shorter than the inverse of the spontaneous emission rate from the upper laser level. Otherwise spontaneous emission will drain the upper level population before a sufficient inversion can be achieved to obtain oscillation.

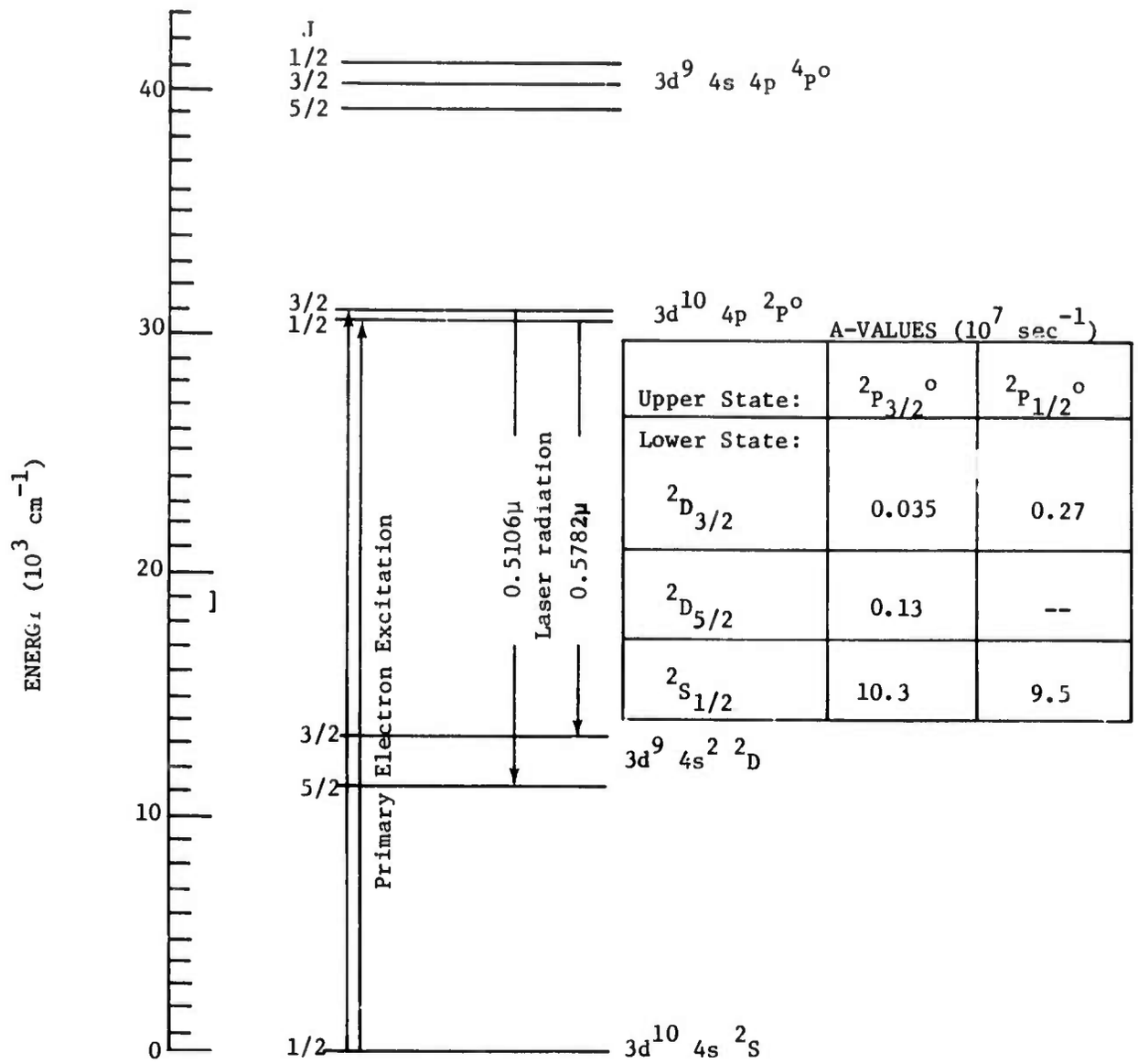

Figure 1. Energy Levels Important to Laser Action in Atomic Copper Vapor

There are several processes which tend to reduce the inversion. The first is, of course, stimulated emission. A second is collisional mixing by electrons between the upper and lower laser level. Bates (6) has given an approximate expression for the ratio of the collisional decay rate between two optically connected atomic levels to the radiative (spontaneous) rate between the same levels. In the case of copper, for an electron density of 10^{14} cm^{-3}, the collisional decay rate is roughly equal to the spontaneous decay rate for the $4s^2\ ^2D_{5/2}$-$4p\ ^2P^o_{3/2}$ transition.

When the upper and lower laser level populations equalize, laser action ceases. In non-flowing systems, relaxation of the metastables at the walls is thought to be the dominant relaxation mechanism in the late afterglow. Decay rates of 2.16×10^3 sec^{-1} and 3.08×10^3 sec^{-1} were found by Chimenti (7) for the $4s^2\ ^2D_{5/2}$ and $4s^2\ ^2D_{3/2}$ levels, respectively, in 2 torr of argon. These rates are slower than the stimulated emission rate by roughly a factor of 10^4. Since a subsequent excitation pulse cannot be applied to the vapor until the metastables are depopulated, a limitation is imposed on the pulse repetition rate, hence, the average power.

B. Copper Vapor Generation

There have been a variety of techniques utilized to generate copper vapor both under equilibrium as well as non-equilibrium conditions. These techniques are listed in Table I. The particular vapor generation scheme utilized plays a fundamental role both in the overall operating efficiency as well as the long term operation of the device. Utilization of the excitation energy dissipated in the active medium to maintain the device at the operating temperature (self-heating) is the most attractive technique from the practical points of view of efficiency and size and weight.

In the high temperature system the solid copper is placed in the laser tube in the presence of an inert gas. A discharge is operated in the inert gas and the power dissipated serves to heat the gas. Conduction through the gas to the walls increases the wall temperature and subsequently heats, melts, and vaporizes the copper.

Similar processes occur in the case of the copper bearing molecules, albeit at lower temperatures. Plasma electrons created in the pulse discharge then dissociate the molecule. The copper is dissociated in excited states which must relax to the copper ground state before a subsequent discharge pulse can produce a population inversion.

In both the high and low temperature systems, the only vapor containment technique thus far employed is the use of several torr of helium or some other inert gas to slow the axial diffusion of the copper vapor from the hot zone of the laser. This is not really a containment technique but does offer some protection to the cold laser windows.

Table I

COPPER VAPOR GENERATION TECHNIQUES

	Technique	Reference
1.	Evaporation of elemental copper-external heater-non-flowing vapor	TRG (9, 10, 11, 13), Polytechnic Institute of Brooklyn (7, 12), Lebedev (14).
2.	Evaporation of elemental copper-self-heated-non-flowing vapor	Lebedev (14).
3.	Evaporation of elemental copper - external heater flowing vapor	AVCO (15), JPL (16), Gulf Atomic (17), GE (18).
4.	Evaporation of Copper Bearing Molecule - Thermal Dissociation	Exxon (19).
5.	Evaporation of Copper Bearing Molecule - Discharge Dissociation	JPL (8), Westinghouse (20), AFWL (Unpublished).

II. THE HEAT PIPE

A. Vapor Containment and Efficiency

One of the practical problem areas in working with vapors at high temperatures is that of containment. The problem is of particular importance to metal vapor lasers in that the lack of a suitable vapor containment technique directly affects both the operating lifetime and the overall laser efficiency as well.

In the case of a high temperature copper vapor system, the required energy, E_A, to generate a vapor phase atom may be computed from

$$E_A = N_0^{-1} \left\{ \int_{T_i}^{T_M} C_p'(T)dT + L_F + \int_{T_M}^{T_f} C_p''(T)dT + L_V \right\}$$

The first and third expressions in the brackets of the above equation are the integrations of the solid and liquid heat capacities, respectively, over the temperature range from an initial temperature, T_i, through the melting point, T_M, to the final operating temperature T_f. The second and fourth terms are the latent heats of fusion and vaporization, respectively. The values of the parameters required to evaluate the above equation are presented below.

Parameter		Value
$Cp'(T)$	(Joules-kg mole^{-1}-°K^{-1})	$22650.59 + 6280.2 \times 10^{-3}/T$ 298°K < T < 1356°K
$Cp''(T)$	(Joules-kg mole^{-1}-°K^{-1})	31401 1356°K < T
T_M	(°K)	1356
L_F	(Joules - kg mole^{-1})	1.31×10^7
L_V	(Joules - kg mole^{-1})	3.05×10^8
N_0	(atoms - kg mole^{-1})	6.02×10^{26}

The value of E_A can be calculated over the operating range of the laser and be shown to vary between 3.6 ev-atom^{-1} at 1300°C to 3.9 ev-atom^{-1} at the high temperature limit chosen to be 2300°C.

In the case of the low temperature cuprous halide system where the copper vapor is obtained through the discharge dissociation of CuCl vapor, for example, the energy expended to obtain the equivalent CuCl vapor density is roughly 1/8 as large or 0.5 ev-molecule^{-1}. The dissociation energy of the molecule to yield atomic copper and chlorine is reported to range between 3.7 and 3.0 ev. The trimeric form reported for the vapor is neglected since the molecular association energies are probably less than a few tenths of an

electron volt. It can be seen that the energy cost per copper atom in this low temperature system is comparable to that in the pure copper system.

It is clear from an efficiency point of view that a flowing system where the active material is used only once for laser action is the worst case. Each copper atom lost from the laser's active volume, whether in a pure copper or cuprous halide system, requires a new atom to be generated with an energy expenditure of roughly 3.7 ev-atom^{-1}. Furthermore, loss of the copper atom in the metastable state subsequent to laser action represents an additional 1.4 ev-atom^{-1} loss of energy. Therefore for a total energy cost of 7.6 ev-atom^{-1} required to generate and excite the atom, 2.25 ev appears as a laser photon and the remainder, 5.27 ev-atom^{-1}, appears as waste heat. Obviously, both recycling of the copper atoms (either through heat pipe techniques at high temperatures or chemical recombination into a volatile molecule in the lower temperature cuprous halide system) as well as reclamation of the waste heat is essential to obtain the highest overall efficiency.

B. Review of the Operation of the Heat Pipe*

The heat pipe may be most easily visualized as a hollow pipe whose inside walls are comprised of a capillary structure which is saturated, at the operating temperature, by a liquid, called the "working fluid". The working fluid may be liquid or solid at ambient conditions. The heat pipe, when placed in thermal contact with a source of energy, will transport this thermal energy by the vaporization and convection of the working fluid. Each atom or molecule of the working fluid leaves the interior surface of the heat pipe at the thermal source and enters the hollow vapor core of the pipe carrying off the latent heat of vaporization. The energy is transported away from the source region (the evaporator) by the vapor flow. Liberation of the latent heat in the thermal sink region (the condenser) occurs by condensation of the vapor. The axial distribution of temperature and vapor pressure depends in a rather complex way on the specific materials, the geometry of construction, the properties of the working fluid, the boundary conditions at the evaporator and condenser, and the input flux of thermal energy. If the evaporator and condenser temperatures are allowed to "float", the operating temperature and vapor zone length will develop to values determined by the balance between input energy in the evaporator region and rejected energy at the condenser.

Heat pipe operation is obtained when the axial transport of energy is essentially entirely accomplished by the vapor convection of the latent heat of vaporization. This is manifested, under appropriate conditions, by very small axial and radial temperature and pressure gradients within the device. In the case where near isothermal conditions exist, the effective thermal conductivity is large. Heat pipes have been operated in which the effective thermal conductivity is greater, by a factor of 10^3, than a solid copper rod of the same dimensions. This large effective conductivity is the basis for the name "heat pipe".

---

* There is an enormous literature compilation on the heat pipe and heat pipe applications, the availability of which may be obtained from the University of New Mexico, NASA Technology Applications Center, Albuquerque, New Mexico 87106.

Continuous operation is made possible by the capillary structure which comprises the internal walls of the device. A properly chosen capillary pore dimension will insure the return of the liquid working fluid from the condenser region back to the evaporator by the surface tension forces. Capillary action therefore acts as a passive pump to replenish the evaporator with working fluid. In general the selection of the capillary pore dimension is a compromise between the surface tension forces and the oppositely directed viscous drag forces. A necessary condition for steady state operation is that the capillary pumping forces which returns the condensate back to the evaporator equal the viscous drag and any acceleration body forces exerted on the device which tends to impede the condensate return.

A structural failure of the wick or an increase in the input heat flux beyond the amount which can be removed by evaporation of the working fluid will cause a local temperature rise in the evaporator. This will cause a further increase in the evaporation rate and the liquid meniscus will continue to recede into the wick until a local dry spot occurs. The temperature will continue to increase locally until heat pipe action is destroyed.

It should be pointed out that the use of a capillary structure may be employed in a metal vapor system as an aid in the confinement of the vapor and the elimination of material build-up at the ends of the tube without the system acting as a heat pipe. A situation in which this condition arises is when the vapor pressure of the working fluid is below that value for which the conductivity is determined by the vapor flow but rather by the conductivity of the wall material and, perhaps, rediation. Since the device does not operate in the heat pipe mode, the accompanying features of small temperature and pressure gradients are not obtained. The wick structure does, however, prevent the accumulation of the condensate at the ends of the tube.

Further advantages of the heat pipe may be obtained if an inert, non-condensible gas is introduced into the pipe. During the initial phase of operation, the inert gas is swept to the condenser region forming a stagnant gas layer. Heat transfer through this layer is essentially by conduction and is relatively slow compared with the vapor condensation process. Heat transfer control is provided by the variation in the overall vapor zone length with variation in the input heat flux. An increase in the heat flux will cause the vapor pressure to increase and the non-condensible gas zone to contract exposing a large section of condensor. A decrease in heat flux causes an expansion of the gas zone and a reduction of the surface area available for condensation. In the case that the vapor pressure becomes equal to the inert gas pressure, a further increase in heat flux will only increase the rate of evaporation but not the vapor pressure. The highest vapor pressure which can be achieved in the pipe is determined exactly by the inert gas pressure. This property has been used to determine vapor pressure of materials.

The start-up dynamics of the heat pipe are complex because the working fluid, in the case of copper, is initially below its melting point. Applications of thermal energy causes the system temperature to rise, the metal in the evaporator to melt, and the vapor generation and transport in the pipe. The metal adjacent to the evaporator is heated, in part, by conduction through the working fluid, wick, and wall and, in part, by vapor condensation. The molten zone moves away from the evaporator. The high axial conductivity of the liquid metal working fluid and the presence of the non-condensible gas lead to a quite rapid start-up of the heat pipe.

C. The Experimental Device

The heat pipe design considerations for the copper vapor laser were determined by the requirements for a homogeneous copper vapor zone, with small axial temperature and density variations. The vapor flow velocity must be small so that the density can be obtained from the ideal gas law where the static vapor pressure-temperature relation can be used. Basically, then, near static conditions are required. Towards this end, an evaporator length which was a large fraction of the overall vapor zone length was employed. Radiation shields were used to minimize the temperature differences between the condenser wall and environment, thereby reducing radiative losses. The heat flux was kept to a minimum. Finally a tube whose length was much longer than the vapor zone was used to minimize the solid angle through which blackbody radiation losses would occur.

The heat pipe, shown schematically in Figure 2, consisted of a graphite tube with an inside diameter of 2.4 cm, a wall thickness of 0.62 cm, and a length of 125 cm. Tungsten foil was used as a liner material on the inside wall of the graphite tube. The purpose of this was to provide a wetting, non-porous surface along which the molten copper could flow. The tungsten foil was cut 80 cm in length. Thicknesses ranging from 2×10^{-3} cm to 7.5×10^{-3} cm were tried. The foil thickness which was found to be most convenient was 5×10^{-3} cm. Precaution is required in the cleaning, cutting and handling of the foil since it is brittle and will crack if creased. The thicker foil, while less fragile, would not assume the contour of the 2.4 cm diameter tube. Techniques to hold the thinner foil against the graphite tube wall was not necessary because of the resilience of the foil.

The wick was composed of a tungsten screen which was rolled up into three layers and inserted into the tube, inside the foil. Screen mesh sizes including 50, 75, 100, and 150 were tried with wire diameters from 2.5×10^{-3} cm to 7.5×10^{-3} cm. The coarser screens did not spring open to the contour of the inside of the tube while the 150 mesh was not resilient enough. It was found that the 100 mesh size with 5×10^{-3} cm wire diameter worked best. In general the wick structure as used in these experiments were troublesome and the specific problems will be discussed later. Oxygen free, high conductivity copper wire, cut to 2.5 cm lengths, was degreased and loaded in piles distributed along the heat pipe length.

The heat pipe was enclosed in a specially designed oven* shown schematically in Figure 3. The heater element was a graphite cylinder with an axial slot cut almost down the entire length. The inside diameter of the element was 7.6 cm and provided a uniform hot zone of 20 cm. The element was supported by graphite studs held by molybdenum clamps fastened to water-cooled copper electrodes which were sealed with O-rings to the outside jacket. Soft copper tubing was used as the water-cooled power leads. Power was supplied from a 14 kw single phase transformer and variac. The water-cooled jacket was a welded steel cylinder 23 cm in diameter and 112 cm long. A graphite tube 5 cm in diameter and 100 cm long was used as a muffle tube. The entire muffle tube and heater element was surrounded by radiation shields which consisted of a continuous rolled graphite cloth 0.62 cm thick. A boron-

* The oven was built by Astro Industries, Inc.

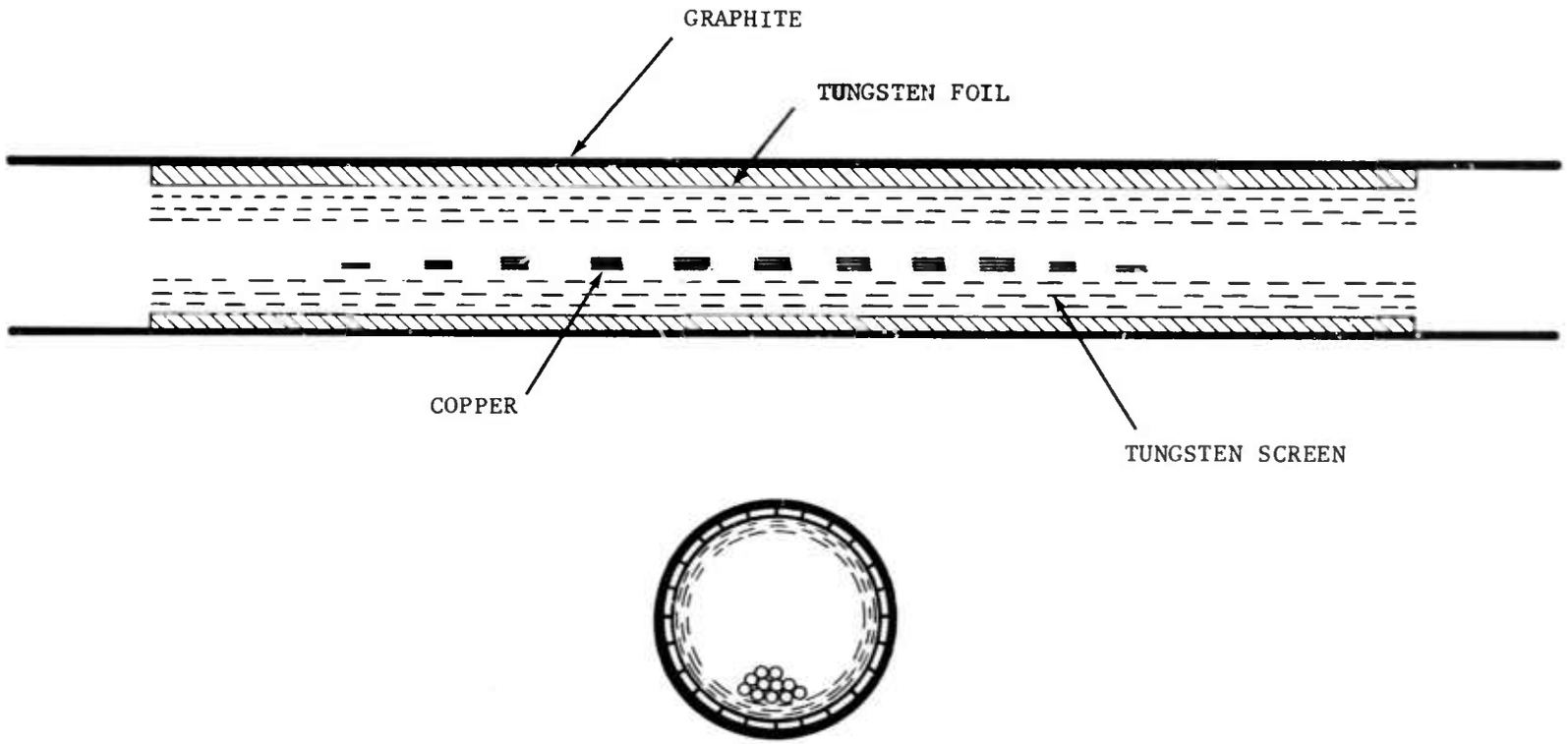

Figure 2. The Heat Pipe Cell

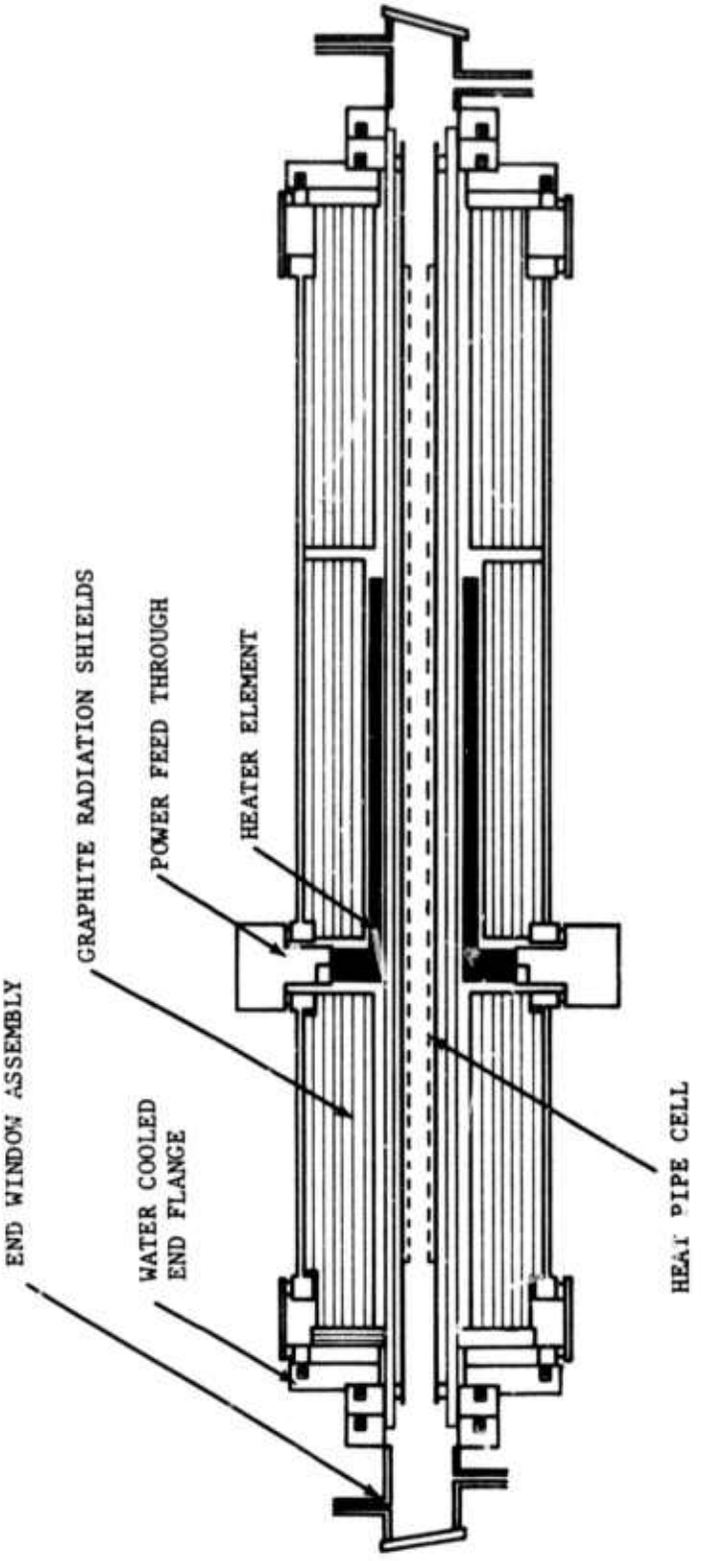

Figure 3. The Heat Pipe Oven

graphite thermocouple was mounted vertically above the center of the hot zone and extended into the oven almost touching the heater element. Two radial sight ports, 2 cm in diameter, were mounted at 180° with respect to each other in the horizontal plane. The thermocouples and radial sight ports were mounted with vacuum O-ring seals and were water cooled. The reported temperatures were measured by an optical pyrometer.

Provision was made for two additional heater elements and thermocouples which could be installed at each end of the device. These heaters would provide two additional 10 cm uniform hot zones, each at a distance of 15 cm from the ends of the large central hot zone. While the mounting flanges were provided on the chamber wall, these heaters were never installed. Provisions for these heaters were made in the event that convection currents in the inert gas regions at each end of the heat pipe would cool the vapor at the vapor-gas interface and thereby cause droplet formation in the volume. In the laser configuration, the scattering losses caused by the droplets would be deleterious to beam quality. The droplet formation was never observed in any of the experiments.

The ends of the cylindrical chamber were sealed with water-cooled, O-ring, bulkhead flanges. Against these flanges were mounted the laser window and electrode assemblies which will be described in Section IV. The heat pipe was supported in these flanges. The interior of the pipe was common with the oven volume. The entire chamber was filled with inert gas and the oven served as a large ballast gas reservoir.

D. Operation of the Heat Pipe

The heat pipe was operated to 2100°C with a copper vapor pressure of approximately 60 torr. Operation in the heat pipe mode became apparent at temperatures of 1500°C and above. This corresponds to a pressure of 0.3 torr. The length of the vapor zone depended on the input heat flux and the inert gas pressure. Typically, a vapor zone length of 60 cm could be maintained at 2000°C at an input power of 2387 watts and with inert gas pressure of 30 torr. An increase in the input power by over 20% to 2850 watts did not increase the heat pipe temperature. A reduction in the confining inert gas pressure by 66% to 10 torr reduced the temperature by 150°C. The vapor zone length in both cases increased to nearly 75 cm.

In 30% of the experiments the device did properly behave as a heat pipe. In all cases but one where the heat pipe failed, the failures could be attributed to an improper functioning of the wick. In the one experiment, the inert gas pressure was set at 8 torr and the power set to 2500 watts. The wick structure appeared to be normal but dry spots were formed near the center of the evaporator and the wall temperature profile became non-uniform.

In the experiments where the wick structure did not function properly, two factors were consistently responsible. The first factor was poor wetting characteristics due to surface contamination of the wick or copper. The screen, foil, and copper had to be carefully degreased. Each time a new graphite tube, radiation shield, heater element or some other component was installed, an extended bake-out at temperatures to 2000°C was necessary to eliminate volatile impurities and subsequent contamination of the wick. Once

these precautions were properly taken, the contamination problem was usually avoided. It was observed that perfect wetting did not occur until temperatures of 1400°C were attained. The wetting characteristics were better at lower temperatures if the copper was melted and saturated the wick structure in a hydrogen atmosphere. This was observed in a separate experiment. The reduction of surface oxides in addition to the graphite bake-out eliminated the non-uniform wetting problems.

The factor which was responsible for most of the failures was the lack of structural integrity of the wick. If the individual layers of screen were creased, stretched or in any way slightly deformed so that the separation between layers were not uniform, then wick failure would occur. In the distorted region capilliary action between the layers would be reduced and liquid copper would "puddle up" causing further distortion of the wick. This would continue until the entire aperture of the vapor region in the pipe would be blocked by the distorted wick. This problem would also occur upon thermal cycling of the heat pipe. Cycled operation requiring the structure to undergo the complex start-up and freeze-out dynamics also caused wick distortions which eventually lead to heat pipe failure. The latter problem could be somewhat reduced if the start-up took place over a period of 3 hours or longer with many small power increments.

It is clear that further wick development is required for cyclic operation at these temperatures and pressures with these materials. Diffusion bonding or swaging the screen layers may add sufficient structural integrity that these problems can be avoided.

Axial temperature variations in all the successful heat pipe experiments were at most $\pm$15°C at 2000°C over the entire 60 cm length. In the vapor-gas interface temperature gradients of 200°C-cm^{-1} were observed. The edge of the liquid copper zone in the vapor-gas interface was not diffuse but extremely sharp. The radial temperature distribution outside of the heat pipe was large because of the thick muffle and heat pipe walls. The heater element was typically 300°C hotter than the outer heat pipe surface. Cycled operation with twenty hours operating time was obtained at 2000°C with no loss of copper and no malfunction of the wick. It was apparent that with further wick development, long term, reliable, cyclic heat pipe operation would be possible and would provide an ideal containment technique for high temperature vapor systems.

III. TRANSVERSE DISCHARGE CONFIGURATIO S

The requirements imposed on the discharge configuration for a high temperature copper vapor laser are severe in that it must be compatible with the vapor generation by discharge heating, vapor containment by heat pipe action, long term operation, and able to produce optimal plasma conditions for efficient excitation of the vapor. While the design features which simultaneously satisfy the above requirements may, in principle, be determined, the operating conditions of the laser present considerable difficulties to the physical realizability of the structure. The extremely high operating temperatures severely restricts the available materials and construction techniques, while thermal efficiency considerations prevent the utilization of discharge configurations which do not serve to minimize thermal losses.

Non-optimized versions of both conventional longitudinal as well as transverse discharge configurations have been applied to high temperature copper vapor lasers. The longitudinal configuration has been the most convenient for systems in which the copper vapor does not flow. The copper vapor is necessarily contained within laser tubes with electrically insulating walls such as oxide ceramics. Precautions must be taken to prevent the liquid copper in the hot zone of the laser from forming continuous liquid filaments which will serve to "short" the discharge. A particular advantage of this configuration is that the electrodes are not brought into the laser volume through the high temperature side walls but rather through the ends of the laser tube which are lower in temperature and usually water-cooled.

A disadvantage of this configuration is its very limited scalability. An increase in length of the device requires an increase in the applied voltage to maintain the optimal E/n_o ratio. For example, calculations indicate that the optimal $E/n_o \approx 8 \times 10^{-15}$ volts-cm^2. If a copper vapor density of 10^{17} cm^{-3} is to be excited, then under matched conditions, an electric field of 1600 volts-cm^{-1} must be applied between the electrodes. The magnitude of the required voltage for a discharge length greater than approximately 25 cm would exceed the maximum voltage rating of available high voltage circuit components such as transmission lines, capacitors, and thyratrons.

A further disadvantage of the longitudinal discharge configuration is the relatively high impedance presented to the excitation pulse generator. Estimates of the optimum plasma conditions indicate that current densities of the order of 10^3 amps-cm^{-2} are required. The laser structure as well as the pulse generator must have low impedance in order that the rapid development of the high current density discharge be possible. In the case of the longitudinal discharge, the impedance is minimized by providing a close fitting current return path surrounding the laser tube. The laser plasma may then be considered as a slightly lossy central conductor of a coaxial transmission line. The impedance, Z_L, may be approximated by

$$Z_L \propto (\varepsilon_r)^{-1/2} \ln (R_o/R_i) \text{ ohms}$$

where ε_r is the relative permittivity of the medium in the annulus between the conductors and R_o/R_i is the ratio of the outer to inner conductor radii. The

smallest ratio attainable in practice, and hence the lowest impedance, is limited by the mechanical and electrical breakdown strength of the laser tube wall material.

A final disadvantage is that for the particular cylindrical geometry heat pipe developed, the vapor volume is surrounded essentially by a liquid copper surface. The conductive walls of the device excludes the operation of a longitudinal discharge in the volume.

The transverse discharge configuration does not suffer the same limitation in scaling as the longitudinal configuration. The optimal E/n_o ratio in the transverse discharge is independent of the device length. The device may be any length subject, ultimately, to other limitations such as the build-up of the radiation field to the extent that coherent processes affect the laser level populations. The major disadvantage of the conventional transverse discharge configuration is a practical one, specific to its application to high temperature laser media. In particular, the electrical, thermal, and material loss problems associated with having plate or pin electrodes entering the vapor through the heat pipe side walls at the extremely high temperatures exclude these configurations.

A. New Discharge Configurations

A novel class of discharge configurations was developed based upon a coaxial electrode structure in which the excitation pulse propagates along the electrode axis. The discharge, however, occurs transverse to the electrode axis. This configuration provided, in part, the advantage of the longitudinal discharge where the electrodes entered the device through the water-cooled ends, yet presented a low impedance to the excitation pulse generator.

The electrodes were in the form of coaxial cylinders in which the outer electrode served, in all cases, as the anode and was maintained at ground potential. The anode also served as the outer wall of the heat pipe. Three specific electrode geometries were investigated, the cross-sectional views of which are presented in Figure 4. In the cross-section shown in Figure 4 (a), the continuous inner cylinder was the cathode. The annular space between the anode and cathode comprised the discharge volume. In Figure 4 (b) is shown the slotted hollow cathode geometry. The geometry, when operated under the fast pulse excitation required for the copper laser produced a discharge which predominantly filled the interior of the hollow cathode as well as the region in proximity to the slot. A weak discharge was observed in the annular region in between the anode and cathode. The geometry shown in Figure 4 (c) was an important modification of the slotted hollow cathode in which dielectric material was used both in the annular region between the electrodes as well as the interior of the hollow cathode in order to confine the active volume to a discharge channel. This modification served to eliminate the dissipation of energy in regions other than the active laser volume and will be discussed further in Section IVC.

B. Excitation Pulse Generator

Excitation of the laser was provided by a coaxial pulse generator connected to one end of the electrode structures previously described.

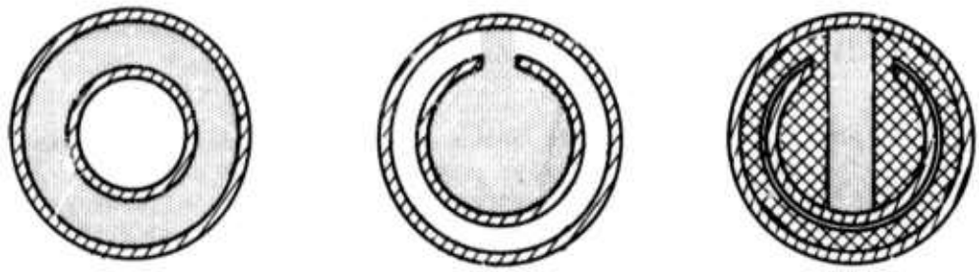

(a) (b) (c)

Figure 4. Cross Sectional Views of Transverse Discharge Electrode Configurations. The electrodes are the concentric cylinders indicated by the diagonal lines. The inner cylinder in each figure is the cathode. The regions in which the discharge occurs are shown as dotted in the figures. The cross-hatched region shown in (c) represents dielectric material.

The circuit diagram for one of the pulse generators which employs resonant charging of the storage capacitors is shown in Figure 5. When series thyratron, T_1, conducts, the dc high voltage supply charges the storage capacitors, C_S, through the charging inductor, L_C, and the diodes, D_1 and D_2. Diode D_1 is a solid state device while D_2 is a vacuum diode. Voltage doubling occurs, across C_S, and the time, t_r, for which the voltage on C_S reaches a maximum is, approximately, assuming loss-less components

$$t_r \approx \pi\sqrt{L_C C_S}$$

When the capacitors are charged the voltage across T_1 falls to zero and the thyratron recovers to its initially non-conducting state. Thus, the series thyratron, T_1, is used to isolate the high voltage supply from the main thyratron when it conducts. The diodes prevent the charge from bleeding off the capacitors before the main thyratron, T_2, is triggered. Therefore, the generator may be operated below the resonant frequency of the charging circuit. A trigger pulse is supplied to the grid of T_2 after a pre-set delay on the delay generator. The shortest delay possible is the recovery time for thyratron, T_1, which is at best 25 μsec. The firing of the main thyratron switches the storage capacitors across the laser tube. The breakdown of the laser medium will be described in the following section.

The portion of the circuit shown enclosed by a dashed line is constructed in a low inductance coaxial configuration, the components of which are shown in Figure 6. The thyratron, plate connection, storage capacitors, and output cathode form the central conductor contained within a coaxial, grounded anode. The diode, D_2, is a vacuum diode which is mounted vertically as shown but within the vertical section of the ground shell. Both forced air and water cooling of the anode shell is provided. Connections to the laser was made either directly or through parallel lengths of coaxial transmission line.

Figure 7 shows the generator driving the laser at a pulse repetition rate of 3×10^3 pulses per second. The larger pulses (100 mv) in the plots represent three consecutive charging current pulses. The peak charging current amplitude is 1A. The four smaller bursts delayed by approximately 180 μsec from the charging pulses are noise generated by the firing of the main thyratron. The applied high voltage was 4 kV and the voltage across the storage capacitor was slightly below 8 kV.

C. Operation of the Discharge

When the thyratron, T_2, in Figure 5, conducts, the voltage builds up across the laser electrodes. A voltage wave propagates down the electrode structure with a velocity, v_p, given by

$$v_p = c\ (\varepsilon_r)^{-1/2}$$

where ε_r is the relative dielectric permittivity of the medium between the anode and cathode. In order to obtain uniform breakdown along the entire

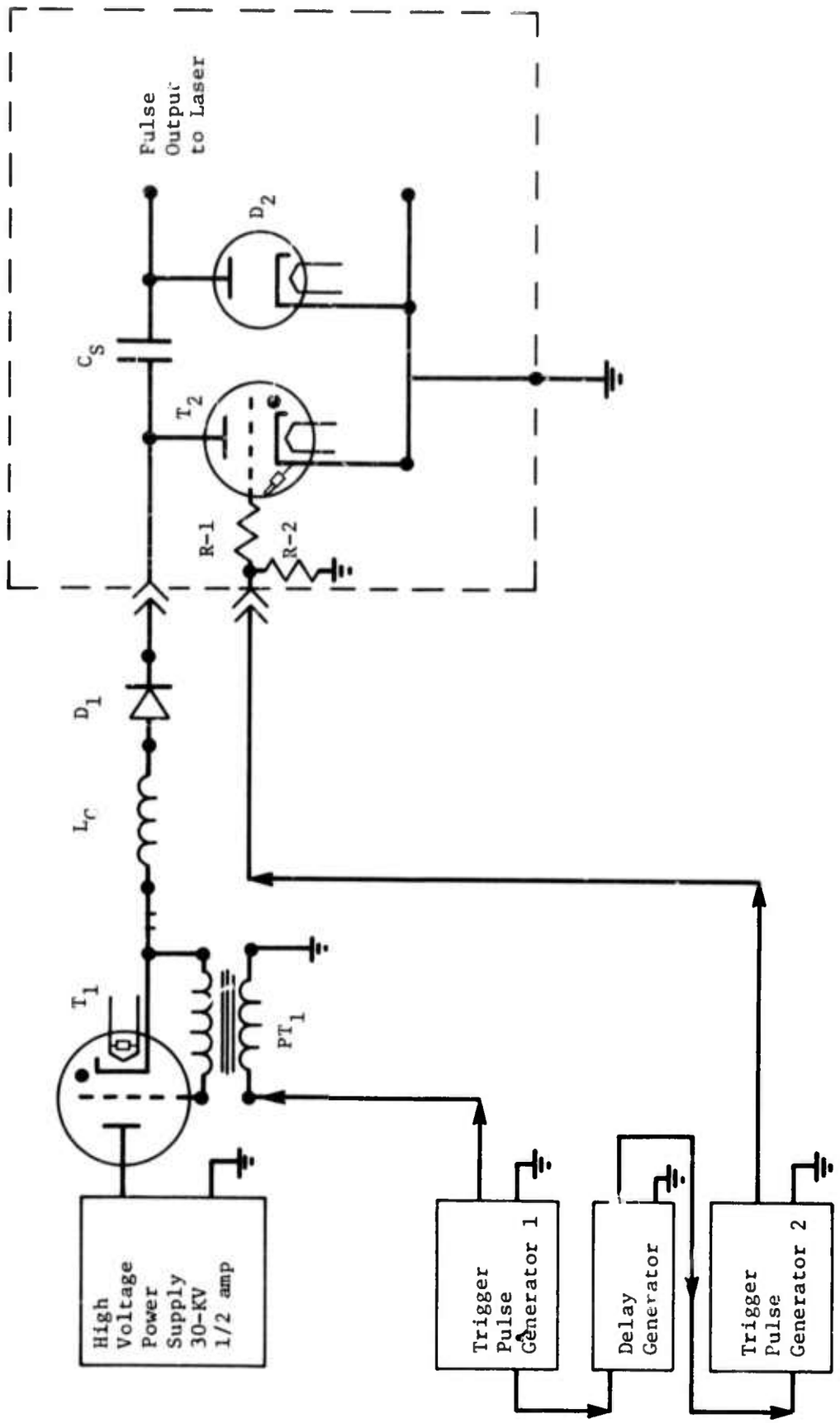

Figure 5. Pulse Generator with Resonant Charging Circuit. Tubes T_1 and T_2 are hydrogen thyratrons (ITT 8613 and F117, respectively); diode D_1 are two silicon rectifiers (EDI-KVP-50); diode D_2 is a vacuum diode (EIMAC 2-240); storage capacitor, C_S, are 16 capacitors (Sprague 30DK-T5) in parallel at 260 pf per capacitor; pulse transformer PT_1 is EGG TR-181; the charging inductor, L_C, is a 6 mh air core inductor built at Exxon.

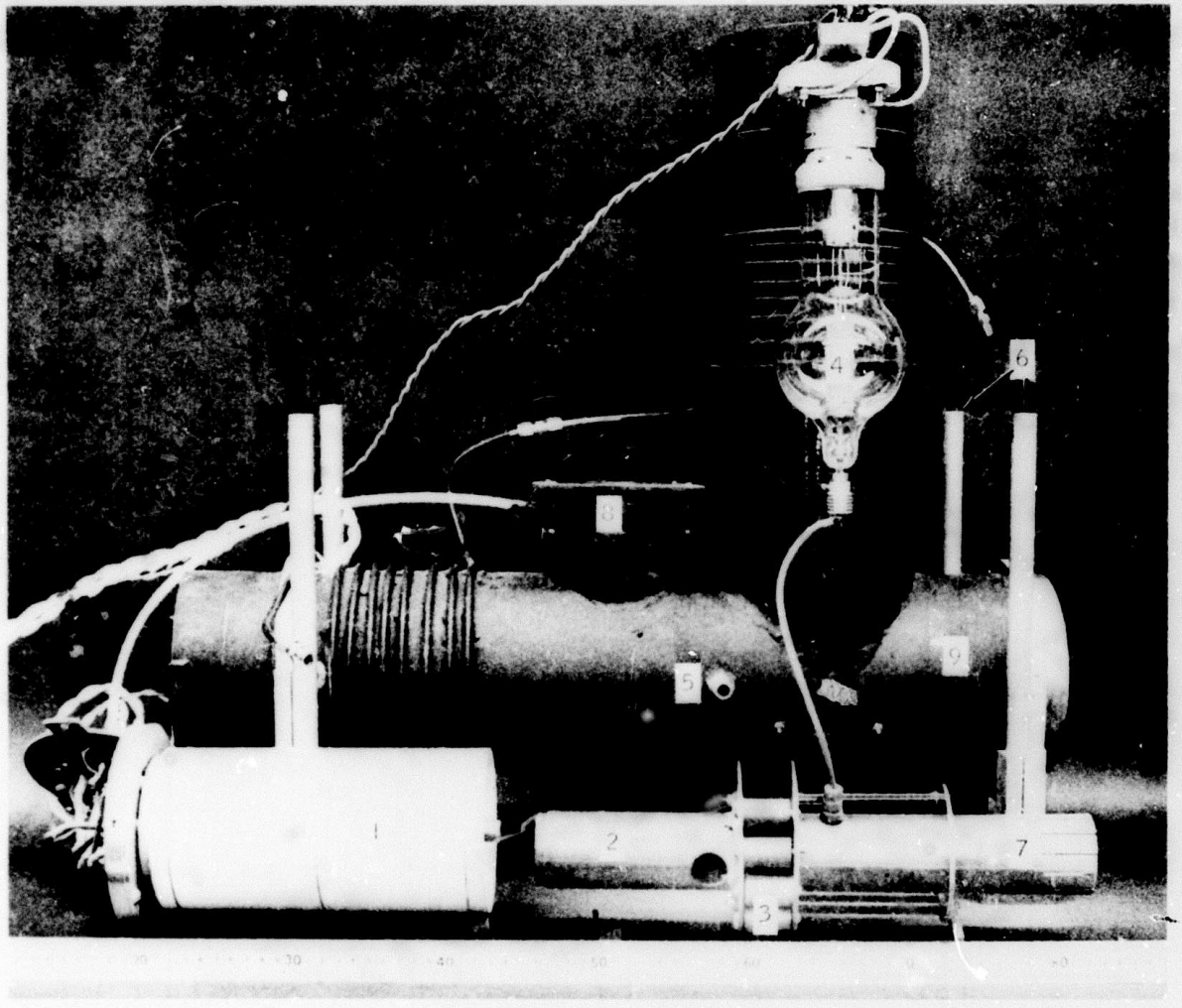

Figure 6. Coaxial Pulse Generator

1. Thyratron; 2. Thyratron plate connection; 3. Storage capacitors; 4. Vacuum diode; 5. High voltage input; 6. Generator support posts; 7. Cathode; 8. Fan; 9. Anode.

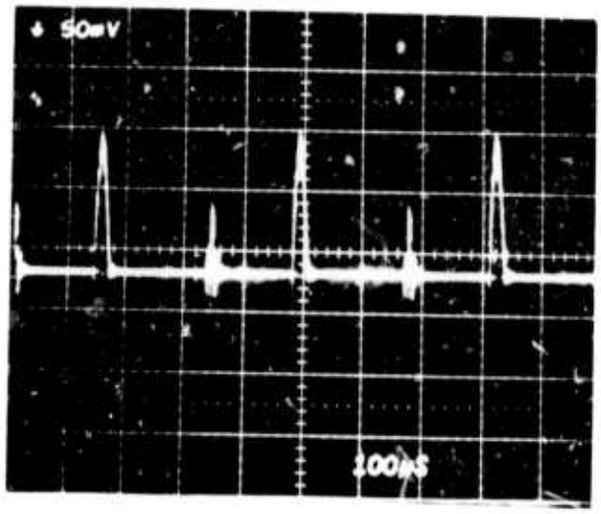

Figure 7. Operation of the Pulse Generator at 3×10^3 pps. The large pulses (at 100 mv level) are three consecutive charging current pulses. The peak charging current is 1 A. The four smaller noise bursts, delayed from the charging pulses by 180 μsec, are generated during the discharge of the storage capacitors into the laser electrode structure.

length of the device, the propagation time of the voltage wave, $\tau p = L/v_p$, should be less than the breakdown time of the medium. This requirement establishes a limit on the device length. If this requirement is satisfied then the active region is overvolted and breakdown occurs simultaneously and uniformly. The shunt conductance of the laser medium subsequent to the breakdown is sufficiently small compared to the series conductance of the electrodes thereby assuring discharge uniformity.

Experiments were carried out to verify that the discharge was, in fact, occuring uniformly along the electrode length. Prototype discharge tubes with geometries shown in Figure 4 (a) and (b) were constructed. The electrodes were copper and the insulating portions Lexan. The anode and cathode diameters were 5 cm and 4 cm, respectively. The length of the discharge tubes were 150 cm. Radial viewing ports were provided in the anode wall at several axial positions along the length of the tube. These ports enabled the discharge light intensity to be monitored. The simultaneous observation of the discharge light intensity from several points along the tube axis was used to verify the simultaneous initiation of the discharge at these points as well as the degree of uniformity of the discharge. The experimental layout is shown in Figure 8. The trigger pulse to the generator was used to trigger the oscilloscope sweep. The applied electric field ranged up to 20 kv-cm^{-1} and argon pressure to 30 torr. To the extent that the spontaneous emission from the discharge yielded a qualitative indication of the spatial and temporal evolution of the initial discharge phases, light from extreme ends of the tube were observed to appear simultaneously ($\pm$ 5 ns) and with the same intensity ($\pm$ 15%). Uniform discharges could not be produced in these prototype devices above 30 torr. Filamentary discharges occurred at apparently random points between electrodes. This was not the case under the high temperature laser operating conditions as will be discussed in Section IV B.

The current risetime in both the prototypes as well as in the laser structure was observed to be shorter than that observed when the pulse generator was terminated in a low inductance short circuit. Current pulse risetimes less than 10 nsec were obtained. This rise time corresponded to the bandwidth limitation of the current probe. An oscilloscope trace of the current pulse is shown in Figure 9. The current pulse is composed of two peaks. The first peak, containing relatively little energy, characteristically exhibits a slower risetime than the second peak. It is believed that the first peak represents the discharge of the capacitance associated with the laser structure. This may be understood from the consideration of an equivalent circuit model of the generator and laser structure shown in Figure 10. The storage capacitor, C_s, is charged to a voltage, V_o, from a high voltage supply. The thyratron switch, SW1, is characterized in its conducting state by resistance, R_s, and inductance, L_s. When the thyratron is fired, SW1 closes and the stored energy is switched across the laser structure. The capacitance associated with the laser structure and connection to the storage element is denoted by C_L. The inductance of the laser and connection to the pulse generator is L_L. When SW1 is closed, the current flow, $i_1(t)$, can be shown to be, assuming an underdamped condition,

$$i_1(t) = (V_o/\omega L) e^{-R_s t/2L} \sin \omega t$$

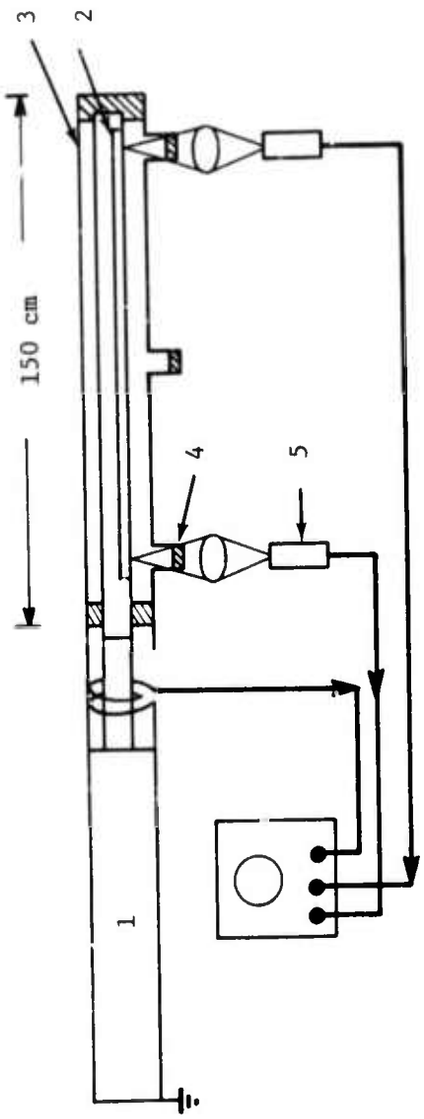

Figure 8. Experimental Arrangement for the Detection of Breakdown Uniformity. 1. Coaxial pulse generator; 2. Slotted hollow cathode; 3. Anode; 4. Window; 5. Photomultiphier.

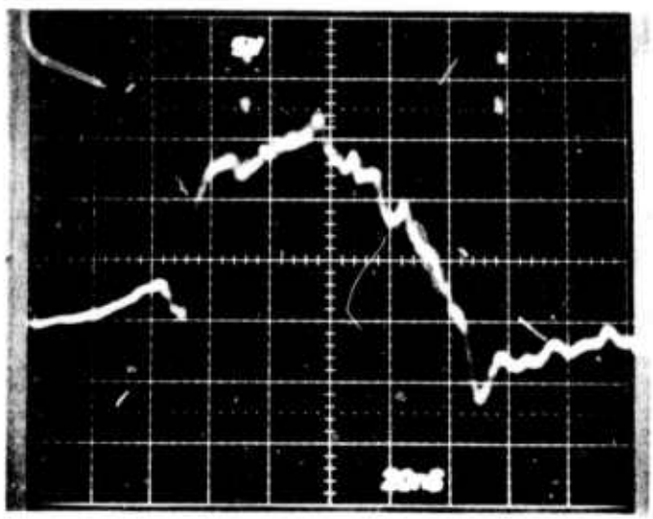

Figure 9. Discharge Current Pulse. The oscilloscope trace shows the discharge current pulse into the prototype laser tube shown in Figure 8. The rise time of the current transformer probe (Pearson Model 411) is 10^{-8} seconds. Vertical deflection: 50 A-div^{-1}; horizontal deflection: 2×10^{-3} sec-div^{-1}.

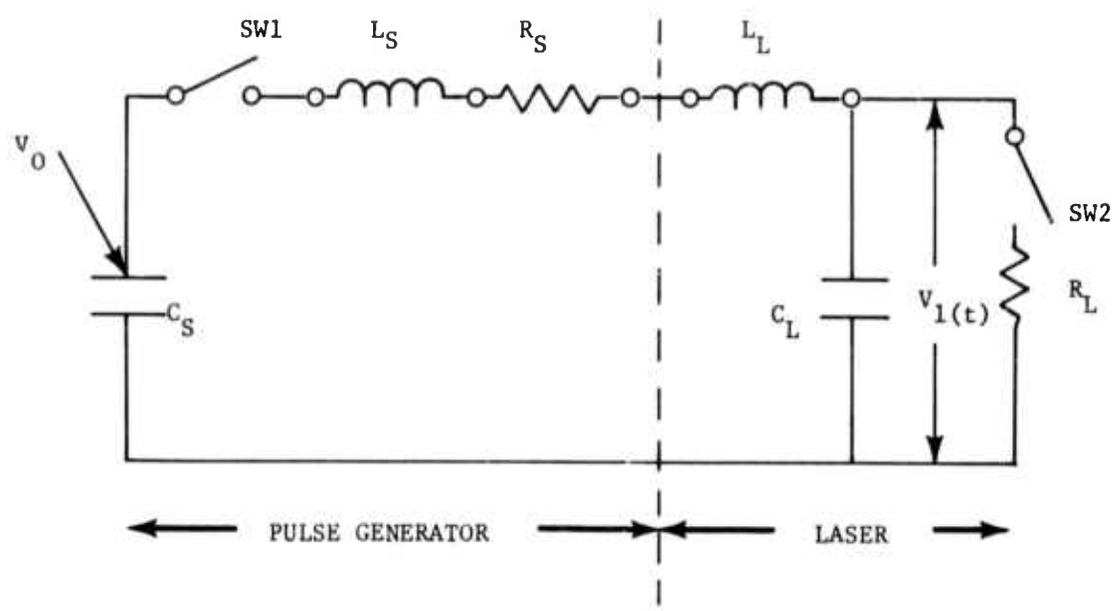

Figure 10. Equivalent Circuit of the Pulse Generator and Laser Discharge. The storage capacitance is C_S. The thyratron, SW1, is characterized, when conducting, by inductance, L_S, and resistance, R_S. The inductance and capacitance of the laser structure and the connection to the generator is denoted by L_L, and C_L, respectively. When breakdown occurs (SW2 closed), the active medium is characterized by resistance R_L.

where $L = L_s + L_L$

$C = C_s C_L/(C_s+C_L)$

and $\omega^2 = (4Z_1^2-R_s^2)/4L^2$ where $\omega^2 > 0$ and $Z_1^2 = L/C$

The voltage $V_1(t)$ which developed across C_L is given by

$$V_1(t) = C_L^{-1} \int i_1(t')\, dt'$$

and can be shown to be

$$V_1(t) = [V_o C_s/(C_L+C_s)] \left\{ (1-e^{-R_s t/2L} \cos \omega t) - (R_s \sin \omega t\, e^{-R_s t/2L})/2\omega L \right\} e^{-R_s t/2L}$$

It can be seen from the above equation that C_L can charge up to a maximum voltage

$$V_1^{max} \approx 2\, V_o C_s/(C_s+C_L)$$

in a time, t_{max}, given by

$$t_{max} \approx \pi/\omega$$

The energy stored capacitatively on the structure is discharged when the breakdown voltage is reached. If the capacitance of the laser structure is equal to the storage capacitance, and if breakdown occurs when $V_1 = V_o$ then the total energy stored on C_s will be discharged through the laser medium. If, on the other hand, only a small fraction of the energy initially stored on C_s is discharged the effect is to preionize the laser medium. The observed short risetime of the main current pulse is believed to be due, in part, to the preionization of the laser medium. The preionization serves to reduce the impedance of the laser structure. This may be understood in the present discharge geometry from the point of view of the addition of a distributed shunt conductance, G, to the lossess coaxial line. In this case the real part of the impedance, Z_R, may be expressed as

$$Z_R \approx \left\{ \frac{\omega^2 LC}{\omega^2 C^2+G^2} \right\}^{1/2} \approx Z_o/\sqrt{1+G^2 Z_o^2}$$

Since $(GZ_o)^2 >> 1$, the real part of the impedance may be approximated as $Z_r \approx 1/G = R_L$. Thus, the discharge of the structure capacitance resulting in

preionization of the laser medium transforms the impedance from that of the initial coaxial structure to the plasma resistance of the active medium.

A second factor which contributed to the fast risetime of the main discharge pulse is that the laser structure capacitance shunts the initial current flow which is determined by the commutation characteristics of the thyratron switch. The inductance of the thyratron drops during its breakdown period due to the fact that the plasma spatially evolves from a thin filament emanating from one of the holes in the grid baffle plate to the full anode diameter. The time for this process to occur is dependent on the hydrogen pressure but is typically 5-30 nsec. From the equivalent circuit point of view the capacitative reactance of the laser structure initially is much less the impedance of the laser medium and shunts the leading portion of the current flow. This occurs until the voltage builds up to the point where the laser medium breaks down and the capacitor discharges as described. The combined effect of the lower thyratron inductance and the lower laser structure impedance results in the short risetime of the main current pulse.

IV. HEAT PIPE COPPER VAPOR LASER

The pulse generator and discharge configurations described in Section III were incorporated with the heat pipe device to demonstrate laser action.

A. The Experimental Device

Laser action was first demonstrated with a hollow cathode structure shown in Figure 4(b). The cathode dimensions were similar to the heat pipe dimensions described in Section II. The cathode was a graphite tube 2.4 cm in diameter with a wall thickness of 0.35 cm and a length of 125 cm. An axial slot of 0.3 cm width was cut into the cathode. The tungsten foil and screen were the same as described in Section II. Care was taken so that the foil and screen did not extend across the cathode slot. Copper was loaded in small piles in the center of the hollow cathode distributed along the heat pipe length.

The graphite muffle tube, which was 5 cm in diameter and 100 cm long was utilized as the anode and maintained at ground potential. The foil and screen wick structure was used as a liner to the interior anode walls. The anode and cathode were physically supported by the heat-pipe oven end-flanges. The laser output end of the device is shown in Figure 11. This flange was all metal and was in electrical contact with the outer oven shell as well as the anode. The cathode was supported in the grounded end assembly by an insulating ceramic disc. The flange was water cooled and had fittings for inert gas flow. A 5 cm diameter quartz flat was used as the output window and was tilted by a few degrees to the optic axis to eliminate feedback.

The electrode flange is shown in Figure 12. Both cathode and anode connections to the pulse generator were made at this flange. Electrical contact to the graphite anode was made by the beveled and locking rings shown in the figure. A brass tube supported and made electrical contact with the cathode. The portions of the flange assembly connected to the anode and cathode were separated by a ceramic disc. A 2.5 cm quartz flat was mounted in a cell at a slight angle (5°) to the optic axis. A brass tube extending over the window supported a mirror mounted so as to reflect the optic axis normal to the heat pipe axis. The reason for this was to permit the coaxial pulse generator to be mounted in line with the heat pipe. This was accomplished by the use of spring fingers on the cathode of the pulse generator or by a locking ring connected to multiple lengths of coaxial cable. In the case of direct contact with the generator cathode, two half-cylinders clamped on to the generator housing and the flange which sealed the electrode assembly to the oven. The high voltage cathode was thereby enclosed. Holes in the half-cylinders for the light beam to emerge and for the glass gas feed and exhaust lines were provided. In the case of the multiple coaxial cable arrangement, one end of the ground braid of each cable was attached to a locking ring on the electrode flange while the opposite end was attached to a locking ring on the generator.

The optical resonator consisted of two plane-parallel reflectors, one was essentially totally reflecting while the output reflector had a dielectric coating with reflectivity at 0.6106μ and 0.5782μ of 85%. The separation between cavity mirrors was 145 cm. A photograph of the laser is shown in Figure 13.

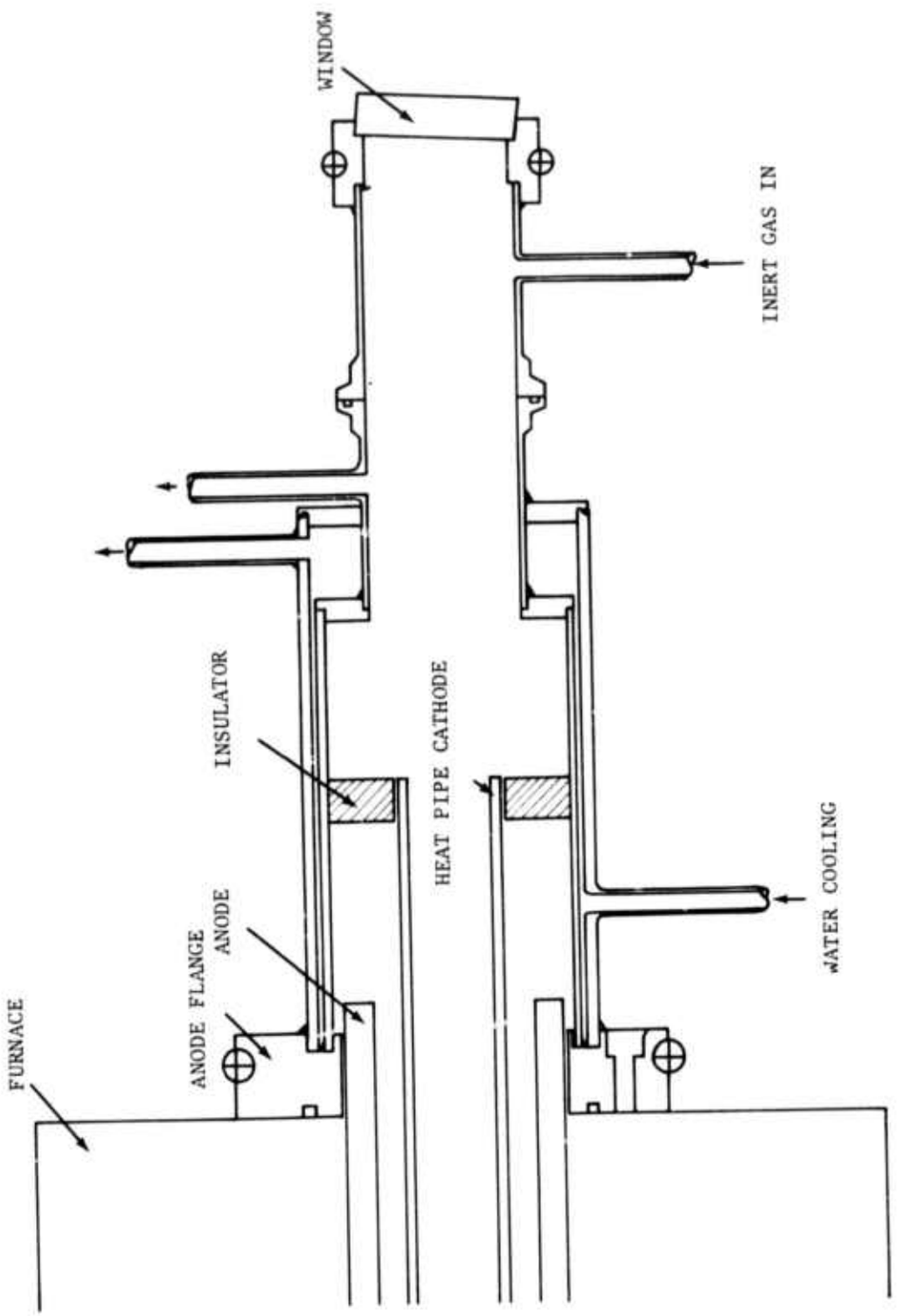

Figure 11. Output Window Flange Assembly

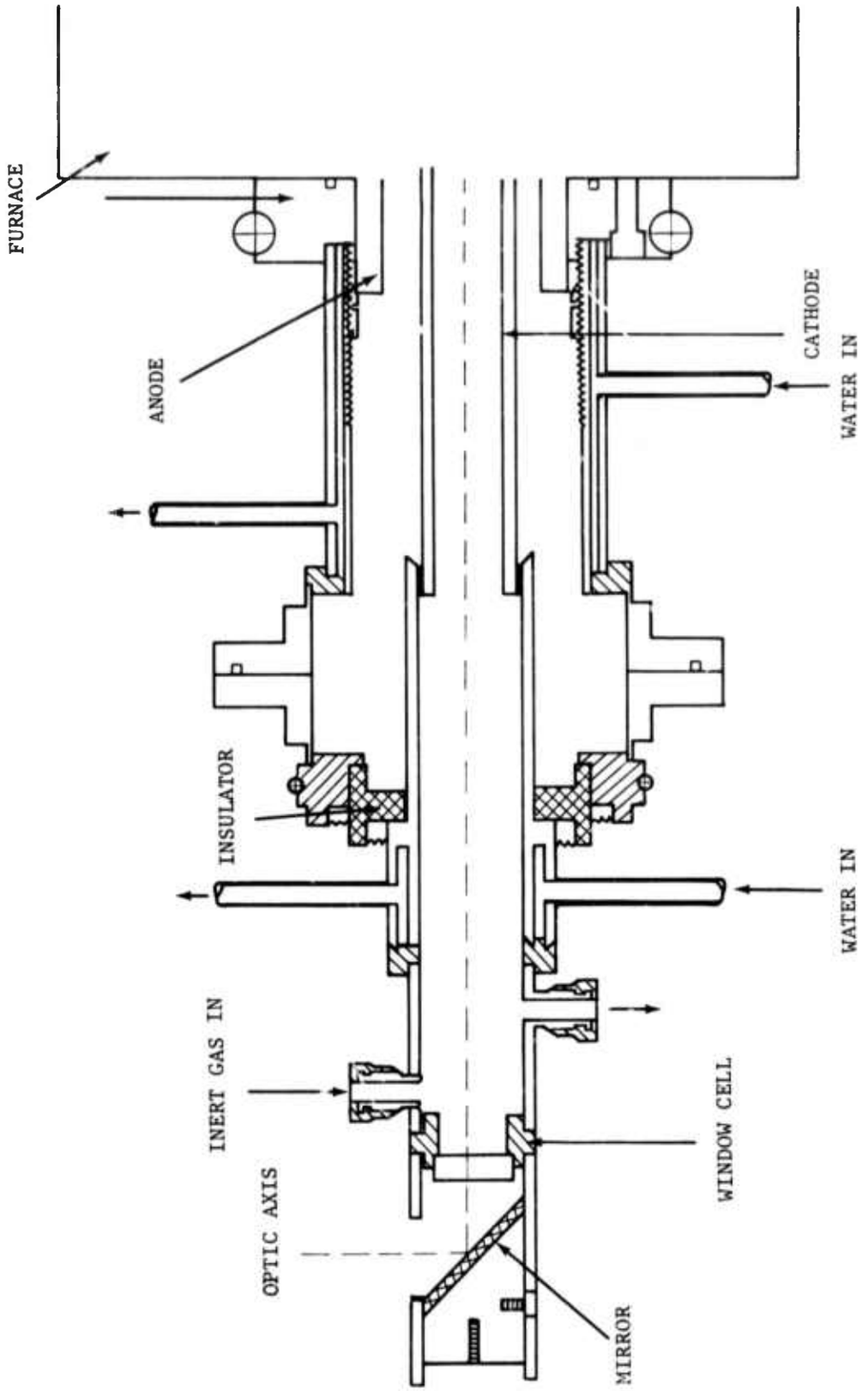

Figure 12. Elecrode Flange Assembly

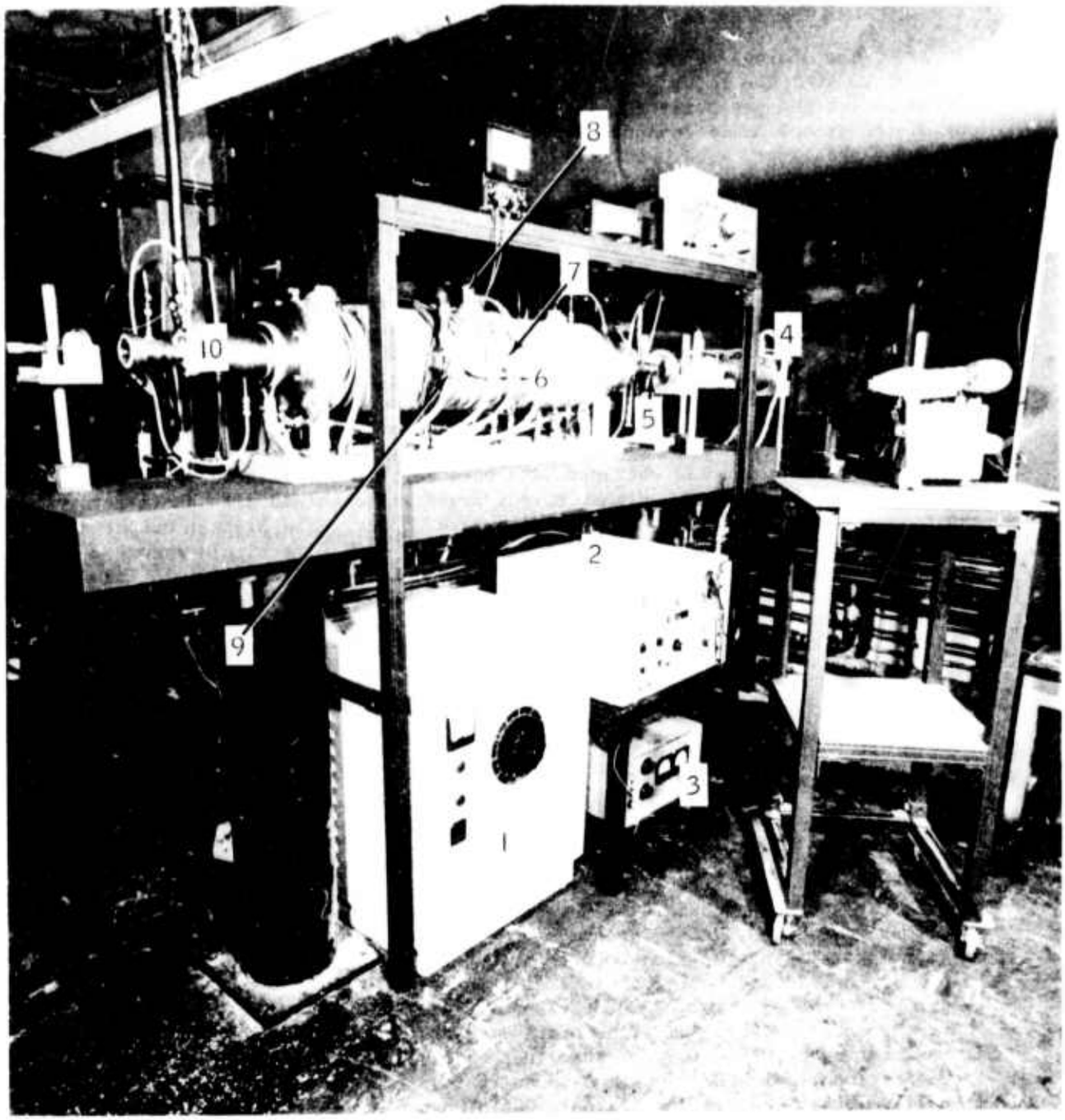

Figure 13. Heat Pipe Copper Vapor Laser.
1. Furnace power supply; 2. Trigger generator; 3. Thyratron filament and reservoir supply; 4. Coaxial pulse generator; 5. Electrode assembly; 6. Heat pipe oven; 7. Radial sight ports; 8. Thermocouple; 9. Oven power feed-through; 10. Output window assembly.

The storage capacitors in the pulse generator were charged to voltages of 20 kv. The actual voltage across the laser tube was not known. The discharge current was monitored inductively by a current transformer surrounding one of the ground braid conductors of the coaxial cables which connected the generator and laser. The bandwidth of the transformer corresponded to a 10 nsec risetime. The measured current risetimes (see Figure 10) were typically 10 nsec and hence bandwidth limited as previously mentioned.

B. Laser Measurements

Laser action was obtained at 0.5106μ in the hollow cathode structure in an operating temperature range between 1500°C and 1900°C. Laser action was also observed at 0.5782μ at temperatures above 1650°C. No successful laser experiments were carried out at temperatures above 1900°C. This temperature corresponds to vapor density of 1.3×10^{17} cm^{-3} and represents what is believed to be the highest copper vapor density in which laser action has been obtained.

Laser action was obtained with pure copper as well as copper-helium and copper-argon mixtures. Higher output power was obtained with an inert gas-copper vapor mixture as compared with pure copper. The highest output resulted with helium. Below temperatures of 1675-1700°C, a single laser pulse was observed to occur during the risetime of the current pulse. The laser pulse width was roughly 5 nsec. Multiple laser pulses during the rise of a single excitation pulse was observed at temperatures between 1700°C and 1900°C. This is shown in Figure 14. The half-intensity width of each component can be seen to be, approximately, 2 nsec and the time between components was 7 nsec. Similar pulses were observed, albeit with significantly reduced intensities, when the output mirror was removed. This may be a manifestation of "gain switching" where by stimulating emission reduces the population difference in a short time due to the initially high gain. The pump rate is sufficiently high to produce a subsequent inversion density.

Previous parametric measurements (7) made on a lower temperature copper vapor laser in a longitudinal discharge configuration have shown that the laser output was substantially reduced at low Cu pressure and for inert gas pressures above 10 torr, presumably due to the fact that the E/n_o ratio was too low. It is significant to point out that laser action has been obtained in the slotted hollow cathode at temperatures above 1800°C and with helium pressures as high as 250 torr and applied voltages of 15 kv. The discharge appeared uniform and filamentary discharges or sparks were not observed. It was mentioned in Section III that in the testing of the prototype discharge configurations, uniform discharges above 25 torr could not be obtained. It is believed that the uniform discharge at high pressure in the laser device was due to the thermionic emission of free electrons by the high temperature electrodes. The density of electrons, n_e emitted at a cathode at elevated temperatures may be shown to be

$$n_e = (2/h^3)\ (2\pi mkT)^{3/2} e^{-\phi/kT}$$

where ϕ is the work function. If we assume that ϕ is of the order of 4 ev and the temperature is approximately 2000°C, the electron density at the cathode structure due to thermionic emission is 10^{12} cm^{-3}. The basic requirement for a uniform discharge is that the electron density at the cathode

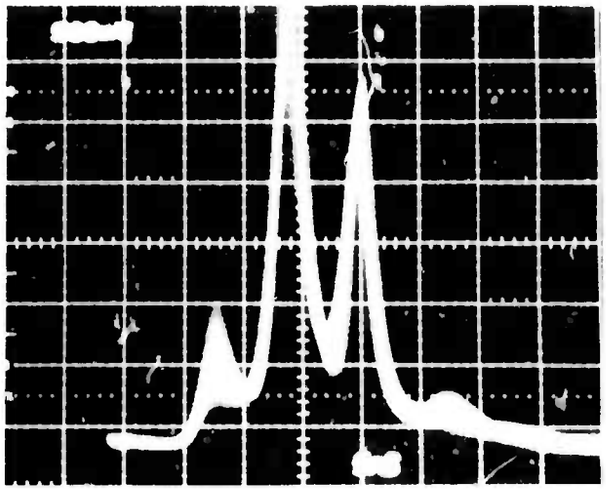

Figure 14. Oscilloscope Photograph Showing Multiple Laser Pulses. Vertical deflection: 1.5 kW-div^{-1}; horizontal deflection: 5 x 10^{-9} sec-div^{-1}. Wavelength is 0.5106μ.

surface be sufficiently high such that the average separation between electrons, $\approx n_e^{-1/3}$, is exceeded by the electron diffusion mean free path, λ_D. Thus $n_e > (\sigma_D n_o)^3$ where σ_D is the diffusion cross-section, taken as 10^{-15} cm^2, and n_o is the total density, taken as 10^{18} cm^{-3} corresponding to 250 torr at 2000°C. The initial electron density at the cathode based upon the above calculation need only be 10^9 cm^{-3}. The thermionic emission is seen to exceed this minimum value and a glow discharge would be expected. Essentially the same numerical results are obtained if the diffusion rate of electrons transverse to the direction of the applied electron field is to exceed the ionization rate. Crudely, these requirements establish a minimum electron density at the cathode for which adjacent avalanche "cones" overlap. Volume ionization is not required.

The excitation volume varied considerably with variation in the copper vapor density. The active volume uniformly filled the center of the hollow cathode in the temperature range from 1500°C to 1600°C. Radiation emerged from the excited region in the cathode slot, as well, and was more intense by typically a factor of three in this temperature range. An increase in the copper vapor pressure caused a gradual contraction of the active volume to the extent that at the high pressure operating limits oscillation was observed only in the cathode slot region. In general, a higher excitation rate would be expected in the slot due to the higher current density and electric field intensity. In addition to the cathode center and slot regions, spontaneous emission from copper vapor which had diffused through the electrode slot could be observed. The cathode support structure at both end-flange assemblies prevented the direct observation of the annular region down the entire heat pipe length.

Several problems were encountered with the laser's operation. The first was that the discharge occuring in the annular region between the electrodes served to reduce the current flow in the active volume. Ideally, all of the discharge current would flow through the cathode slot. Attempts to channel the current flow only through the active volume were made by modification of the electrode structures. This will be described further. A second problem was the accumulation of copper at the edges of the wick structure adjacent to the cathode slot. This served to vary the active volume and in extreme cases obscure the cross section. This latter problem caused considerable variation in the output power. Output power as high as 75 kw was obtained at 1800°C. This power appeared to be generated in the slot region with a volume of approximately 7 cm^3, resulting in an energy density of 50 $\mu J\text{-}cm^{-3}$.

Due to the aforementioned problems, detailed parametric study of the output characteristics with the discharge and vapor density was not made during the time available in favor of attempts to eliminate these problems.

C. Modifications

Modification of the hollow cathode structure was made in an attempt to confine the current flow to the active volume and to increase the current density. Towards this end a dielectric material was used to fill both the annular interelectrode space as well as the wall region in the interior of the hollow cathode. The resultant laser tube cross-section is shown in Figure 4 (c).

The material chosen for this application was boron nitride. Manufacturer claims indicate that it can be used to 3000°C and exhibits a room temperature dielectric strength to 1000 volts-mil^{-1}. The material was thermally shock resistant and easily machinable.

A second heat pipe oven, similar in design and operation as previously described was constructed but with an evaporation length of 4 cm and an overall assembled length of 30 cm. A tube of boron nitride 5 cm in diameter and 30 cm long was machined with the cross-section shown in Figure 4 (c). The discharge channel width was 1 cm and height was 4 cm. The length of the vapor zone was 10 cm. The discharge channel was cut through the outer wall of the boron nitride for a length of 10 cm corresponding to the vapor zone. The active discharge volume, then, was 40 cm^3. An annular sector with an outside diameter of 4.36 cm and an inside diameter of 4 cm was cut into the boron nitride tube. A tungsten foil and wick structure was inserted along the entire length of the tube and connected to the cathode portion of the electrode flange. Tungsten foil was wrapped around the outside of the boron nitride and enclosed within a graphite cylinder. The tungsten and graphite made electrical contact with the anode portion of the electrode flange and this combination served as the anode. The boron nitride laser tube mounted in the electrode flange is shown in Figure 15.

Room temperature experiments with the discharge indicated currents of 2 x 10^{3}A with less than 15 nsec risetime were obtained. All of the current flow was in the 10 cm^2 channel cross section. Subsequent experiments at high temperature (to 1800°C) in the heat pipe section showed that no breakdown in the 0.32 cm thickness of boron nitride occured at voltages to 20 kV.

Laser action was obtained in the temperature range from 1500°-1550°C. Considerable vaporization of volatile material from the boron nitride resulted in the failure to obtain laser action above 1550°C. Alteration of the discharge characteristics and the tremendous scattering losses due to the vapor phase condensation of volatile foreign species in the ends of the heat pipe were principally responsible for the inability to obtain laser action. In addition, condensation of the materials at the ends of the wick structure changed the wetting characteristics and eventually destroyed the heat pipe action.

Elemental analysis of the white crystals and powder obtained upon the cooling down of the device indicated that the crystals were composed of boron (>10%), magnesium and calcium (1-10%), nitrogen (1.8%). The powder had a higher calcium content consisting of boron and calcium (>10%), magnesium (1-10%), and nitrogen (3.5%). Trace metals were found in both cases. Efforts were made to reduce the volatile species by extended high temperature bake out under vacuum. No significant improvements were obtained. Use of other grades of boron nitride were not tried. This problem remained unresolved at the end of the program.

Figure 15. Boron Nitride Laser Tube and Electrode Flange. (1) Boron nitride laser tube with slot in the active region. A graphite anode with tungsten foil as a liner fits tightly around the boron nitride tube. Electrical contact is made at the water cooled anode flange (2). The crescent-shaped (see Figure 4 (c)) graphite cathode with the tungsten foil and screen wick structure makes electrical contact at (4), the water cooled cathode ring. The ports through which the inert gas flows may be seen. The window cell is sealed with o-rings to the threaded portion of the cathode ring. The ceramic spacer (3) is epoxied to the boron nitride tube. The seal cannot be seen in the photograph. The discharge occurs through the slot between the anode and cathode. The slot width is 1 cm and length is 10 cm.

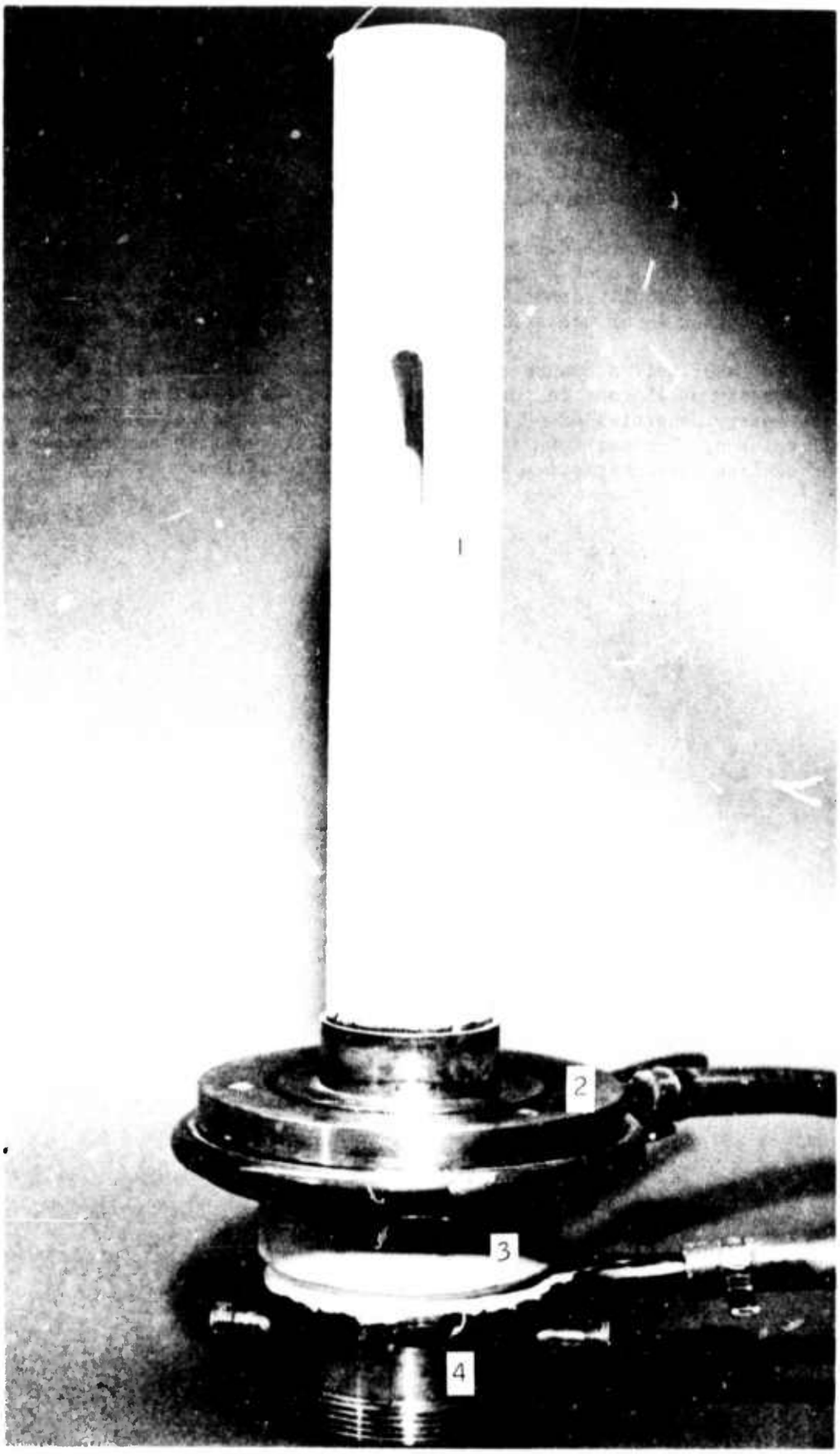
1
2
3
4

V. CONCLUSIONS

The containment of copper in a heat pipe at temperatures to 2100°C and vapor pressure control by helium and argon have been obtained. While further work is required to improve the structural integrity of the wick under thermal cycling, this technique provides a straightforward way to contain and control high temperature metal vapors.

New transverse discharge configurations have been developed which enabled the production of high current, short risetime excitation pulses in laser tubes with electrically conducing walls. These configurations may be applied to other laser media in which fast pulse excitation is required.

Laser action has been demonstrated in a heat pipe with a copper vapor density of 15 torr in pure Cu and with helium pressures to 250 torr. Output energy densities of 50 $\mu J\text{-}cm^{-3}$ have been observed at 0.5106μ in small volumes. Further work is required to obtain optimum performance and power scaling characteristics at higher copper densities.

BIBLIOGRAPHY

1. Corliss, C. H., and Bozman, W. R., Experimental Transition Probabilities for Spectral Lines of Seventy Elements, NBS Monograph 53, 1962.

2. Holstein, T., "Imprisonment of Resonance Radiation in Gases", Phys. Rev., 72, 1212, 1947.

3. Massey and Burhop, Electronic and Ionic Impact Phenomena, Oxford Press (1952).

4. Leonard, D. A., "A Theoretical Description of the 5106Å Pulsed Copper Vapor Laser", IEEE J. of Quant. Elect., QE-3, 380, (1967).

5. Williams, W., and Trajmar, S., "Elastic and Inelastic Electron Scattering at 20 and 60 eV from Atomic Cu", Phys. Rev. Lett., 33, 187 (1974).

6. Bates, D. R. Atomic and Molecular Processes, Academic Press, p. 262, (1962).

7. Chimenti, R. J. L., "The Copper Vapor Laser" Ph.D. Thesis, Polytechnic Institute of Brooklyn, (1972).

8. Chen, C. J., Nerheim N. M., and Russell, G. R., "Double-Discharge Copper Vapor Laser with Copper Chloride as a Lasant", Appl, Phys. Lett., 23, 514, (1973).

9. Walter, W. T., Piltch, M. Solimene, N. and Gould, G., "Pulsed Laser Action in Atomic Copper Vapor", Bull. Am. Phys. Soc., Ser. II, 11, 113, (1966).

10. Walter, W. T., "40-kW Pulsed Copper Laser", Bull. Amer. Phys. Soc., Ser. II, 12, 90, (1967).

11. Walter, W. T., "High Power Copper Laser", Final Report, NADC Contract No. N62269-3584, July (1966).

12. Chimenti, R. J. L. and Walter, W. T., "Coherence Properties of the Pulsed Cu Vapor Laser", Bull. Am. Phys. Soc., Ser. II, 16, 41, (1971).

13. Piltch, M., amd Gould, G., "High Temperature Alumina Discharge Tubes for Pulsed Metal Vapor Lasers", Rev. Sci. Inst., 37, 925, (1966).

14. Isaev, A. A., Kazaryan, M. A., and Petrash, G. G., "Effective Pulsed Copper Vapor Vapor Lesser with High Average Generation Power", JETP Letters, 16, 27 (1972).

15. Leonard, D., "Airborne Laser Development", Final Report, Avco Everett Research Laboratory, DAHC 60-70-C-0030, September, 1970.

BIBLIOGRAPHY
(Contd)

16. Russell, G. R., Nerheim, N. M., Pivirotto, T. J., "Supersonic Electrical Discharge Copper Vapor Laser" Appl. Phys. Lett., 12, 585 (1972).

17. Asmus, J. and Monocur, N., "Exploding Wire Cu Vapor Laser", Appl. Phys. Letters, 13, 384 (1968).

18. Karras, T. W., Anderson R. S., Bricks, B. G., Buczacki, T. E., and Springer, L. S., "Copper Vapor Generator", Final Report, Contract F29601-72-C-0079, Air Force Weapons Laboratory, Technical Report No. AFWL-TR-73-133 (1973).

19. Chimenti, R. J. L., "Efficient, Low Temperature, Copper Vapor Generator", Final Report, Contract No. F29601-72-C-0081, Air Force Weapons Laboratory, Technical Report No. AFWL-TR-73-95 (1973).

20. Weaner, L. A., Liu, C. S., and Sucov, E. W., "Superradiant Emission at 5106, 5700 and 5782 Å in Pulse Copper Iodide Discharges", IEEE J. of Quant. Elect: QE-10, 140 (1974).

21. Schuebel, W. K. Appl. Phys. Litt. 16 470 1970.